Spatial Non-Uniformities in $[Ca^{2+}]_i$ during Excitation-Contraction Coupling in Cardiac Myocytes

M. B. Cannell,* H. Cheng,‡ and W. J. Lederer‡

*Department of Pharmacology and Clinical Pharmacology, St. George's Hospital Medical School, London SW17 0RE, United Kingdom; and ‡Department of Physiology and the Medical Biotechnology Center, University of Maryland at Baltimore School of Medicine, Baltimore Maryland 21201 USA

ABSTRACT The intracellular calcium ($[Ca^{2+}]_i$) transient in adult rat heart cells was examined using the fluorescent calcium indicator fluo-3 and a laser scanning confocal microscope. We find that the electrically evoked $[Ca^{2+}]_i$ transient does not rise at a uniform rate at all points within the cell during the $[Ca^{2+}]_i$ transient. These spatial non-uniformities in $[Ca^{2+}]_i$ are observed immediately upon depolarization and largely disappear by the time the peak of the $[Ca^{2+}]_i$ transient occurs. Importantly, some of the spatial non-uniformity in $[Ca^{2+}]_i$ varies randomly in location from beat to beat. Analysis of the spatial character of the non-uniformities suggests that they arise from the stochastic nature of the activation of SR calcium-release channels. The non-uniformities in $[Ca^{2+}]_i$ are markedly enhanced by low concentrations of Cd^{2+}, suggesting that activation of L-type calcium channels is the primary source of activator calcium for the calcium transient. In addition, the pattern of calcium release in these conditions was very similar to the spontaneous calcium sparks that are observed under resting conditions and which are due to spontaneous calcium release from the SR. The spatial non-uniformity in the evoked $[Ca^{2+}]_i$ transient under normal conditions can be explained by the temporal and spatial summation of a large number of calcium sparks whose activation is a stochastic process. The results are discussed with respect to a stochastic local control model for excitation-contraction (E-C) coupling, and it is proposed that the fundamental unit of E-C coupling consists of one dihydropyridine receptor activating a small group of ryanodine receptors (possibly four) in a square packing model.

INTRODUCTION

The contraction of heart muscle is activated by an increase in the free intracellular calcium concentration ($[Ca^{2+}]_i$) that is due to calcium influx across the sarcolemma (SL) as well as calcium release from intracellular stores (see Wier (1990) for review). The majority of the calcium that activates contraction comes from the sarcoplasmic reticulum (SR) and the release of this calcium is "triggered" by the SL calcium influx via a process known as "calcium-induced calcium release" (CICR) (Fabiato, 1985a,b; see Callewaert (1992) for review). Thus the sarcolemmal calcium influx (due to the calcium current as well as the Na/Ca exchanger) is amplified by the CICR mechanism to provide sufficient calcium to activate the contractile proteins. Amplification of an increase in $[Ca^{2+}]_i$ by CICR is a positive feedback system, which is therefore potentially unstable. However, under normal conditions the release of calcium by the SR is completely graded (Cannell et al., 1987a,b; Beukelmann and Wier, 1988; Callewaert et al., 1988; duBell and Houser, 1989).

Whereas graded release of calcium would be explainable by a low-gain system, some features of calcium release from the SR were indicative of a high-gain system (Cannell et al., 1987b). This apparent variation in gain led to the suggestion that a simple CICR mechanism (where calcium release depends only on the spatial averaged calcium influx and $[Ca^{2+}]_i$) could not explain the regulation of SR calcium release (Cannell et al., 1987b; Wier et al., 1994). To reconcile a variable gain system with CICR, it has been suggested that the spatial organization of the SR release channels may play a critical role in excitation-contraction (E-C) coupling (Niggli and Lederer, 1990a; Wier et al., 1994). SR release can be terminated once it has started by switching off the calcium current (Cannell et al., 1987b; Cleeman and Morad, 1991; Wier et al., 1994), which is difficult to reconcile with simple CICR models (Cannell et al., 1987b), a view supported by the recent results of Wier et al. (1994). Mathematical modeling also suggested that calcium release from the SR was not explainable by a simple CICR mechanism unless the model also included stochastic gating of spatially organized SR release sites (Stern, 1992). Thus, although the relationship between the spatial averaged $[Ca^{2+}]_i$ and the calcium current has been taken to support simple (mass action) CICR models (e.g., Callewaert, 1992), more detailed analysis suggests that CICR from the SR requires additional factors that introduce nonlinearities in the transfer function between $[Ca^{2+}]_i$ and SR calcium release (such as stochastic channel gating (Stern, 1992); and/or small diffusional spaces (Niggli and Lederer, 1990a)).

There is a nonlinear relationship between the peak of the $[Ca^{2+}]_i$ transient and the calcium current (Cannell et al., 1987a,b; Callewaert et al., 1988; duBell and Houser, 1989). However, Callewaert et al. (1988) proposed that the relationship between the calcium current and SR calcium release should be measured during the rising phase of the $[Ca^{2+}]_i$ transient, and the resulting linear relationship between the calcium current and $[Ca^{2+}]_i$ has been taken as evidence in

Received for publication 23 March 1994 and in final form 17 August 1994.

Address reprint requests to W. J. Lederer, Department of Physiology and the Medical Biotechnology Center, University of Maryland at Baltimore School of Medicine, 660 W. Redwood St., Baltimore, MD 21201. E-mail: wlederer@umab.umd.edu.

0006-3495/94/11/1942/15 $2.00

support of a simple CICR model where the SR release channel is tightly coupled to a sarcolemmal calcium channel (see Callewaert, 1992). However, biochemical evidence does not support a 1:1 relationship between sarcolemmal calcium channels and SR release channels (Bers and Stiffel, 1993). In addition, models of this type (which are inherently low gain with respect to spatially averaged cytosolic $[Ca^{2+}]_i$) will not predict propagating CICR (or calcium waves), because they assume that the SR release channel is quite insensitive to cytosolic calcium. The latter assumption is required to enable control only by the local calcium concentration (which is determined by the calcium influx via the sarcolemmal calcium channels during activation) to prevent non-graded regenerative behavior. More recently, Wier et al. (1994) reported that the relationship between calcium release and calcium current was very nonlinear and suggested that magnitude of the voltage-dependent calcium influx via single calcium channels is a critical factor in determining calcium release from the SR.

It is possible that the reported differences in the relationship between the calcium current and $[Ca^{2+}]_i$ (see above) may be partly explained by changes in the spatial distribution of $[Ca^{2+}]_i$ during the rising phase of the $[Ca^{2+}]_i$ transient. $[Ca^{2+}]_i$ must be non-uniform (at least at the subsarcomeric level) during the rise in $[Ca^{2+}]_i$ (Cannell and Allen, 1984; Wier and Yue, 1986), and this is a potentially serious problem for analysis of CICR, because a nonlinear relationship between calcium current and SR calcium release will not be defined by the relationship between spatial averaged $[Ca^{2+}]_i$ and calcium current (for the same reasons that a nonlinear indicator does not correctly report spatial averaged $[Ca^{2+}]_i$; see Yue and Wier (1985)).

Real-time examination of the properties of SR calcium release channels in intact heart muscle cells was made possible recently using confocal microscopy and the calcium indicator fluo-3 (Cheng et al., 1993). This work, examining calcium sparks (which arise from the spontaneous opening of SR calcium release channels) provided evidence that CICR is not particularly sensitive to $[Ca^{2+}]_i$ under resting conditions (as suggested by Niggli and Lederer, 1990a) so that propagating waves of CICR do not normally occur. A similar conclusion was reached by Trafford et al. (1993). In this paper we examine the spatial uniformity of calcium transients evoked by electrical stimulation and, for the first time, show that the activation of SR calcium release by depolarization is not spatially uniform. In addition, we examine the relationship between calcium sparks and the normal calcium transient and the extent to which the observed local non-uniformities in $[Ca^{2+}]_i$ can be explained by stochastic gating of channels involved in excitation-contraction coupling.

MATERIALS AND METHODS

Cells

Single rat cardiac myocytes were dissociated by enzymatic treatment as described elsewhere (Cheng et al., 1993; Mitra and Morad, 1985). Aliquots of cells were exposed to 5 μM fluo-3 AM (diluted from a stock containing 50 μg Fluo-3 AM, 25 μg Pluronic (Molecular Probes, Eugene, OR) in 100 μl dimethyl sulfoxide) for 5 min followed by a 30-min wash in extracellular solution to allow time for deesterification.

Solutions

The standard bathing solution contained (in mM): 137 NaCl, 5.4 KCl, 1.2 $MgCl_2$, 1 $CaCl_2$, 20 HEPES (pH = 7.4 at 25°C). $CdCl_2$, 2,3-butanedione monoxime (BDM) (Sigma Chemical Co., St. Louis, MO), thapsigargin (Sigma Chemical Co.) and ryanodine (S. B. Pennick and Co., New York) were added to the standard bathing solution as needed. Control experiments showed that BDM had no effect on the fluorescence of fluo-3.

Confocal microscope

A modified Biorad MRC 600 confocal scanning head was attached to a Nikon Diaphot microscope. A Zeiss Neofluor 63× 1.25 N.A. objective lens was used in most of the experiments; other experiments used a Nikon Neofluor 40× 1.3 N.A. objective. The confocal detector aperture was set to 75% of maximum, providing an axial (z) resolution of 0.8 μm and x-y resolution of just under 0.4 μm as measured at full width at half maximal with 0.1-μm fluorescent beads (Molecular Probes, Eugene, OR). Illumination was provided by a 20-mW Argon ion laser (Ion Laser Technology, Salt Lake City, UT) whose illumination intensity was set by selectable neutral density filters. The excitation wavelength (488 nm) was selected using interference filters.

Cells were electrically stimulated with 2-ms voltage pulses delivered through parallel platinum wires. The stimulation voltage was set to 1.5 times threshold. The stimulation pulse was triggered by the confocal scan at a selectable line and pixel. The exact timing of the stimulation was marked in the image by triggering a light-emitting diode mounted near the MRC 600 photomultiplier detector to flash for 1 μs. This marked the stimulation time by briefly saturating the photomultiplier output signal (for one pixel).

Image analysis

The confocal microscope interface was hosted by a 66-MHz 486 computer (Gateway 2000, N. Sioux City, SD) and data files were archived in a 600-MB rewritable optical cartridge. Image processing was performed on an IBM RS/6000 workstation (IBM, Boca Raton, FL) running IDL software (Boulder, CO). Final images were photographed directly from the computer monitor.

Calcium concentration calibration

The time course of the $[Ca^{2+}]_i$ transient can be estimated from the fluorescence record, given the following:

$$[Ca]_i = K\frac{(F - F_{min})}{(F_{max} - F)} \quad (1)$$

where K is the affinity of the indicator for calcium, F_{min} the fluorescence in the absence of calcium, and F_{max} the fluorescence in the presence of saturating calcium (Grynkiewicz et al., 1985).

For fluo-3, $F_{min} \sim 0$ so that F_{max} can be estimated from the resting level of $[Ca^{2+}]_i$:

$$F_{max} = F_{rest}\left(\frac{K}{[Ca]_{rest}} + 1\right) \quad (2)$$

An estimate of the time course of the $[Ca^{2+}]_i$ transient can be made from the fluorescence record by dividing Eq. 1 by F_{rest} and substituting Eq. 2 for F_{max}:

$$[Ca]_i = \frac{KR}{K/[Ca]_{rest} - R + 1} \quad (3)$$

where R is the "normalized fluorescence" signal (F/F_{rest}). It was assumed

that $[Ca^{2+}]_i$ at rest was close to 100 nM as shown in other studies (e.g., Cannell et al., 1987b; Allen et al., 1984; Wier et al., 1987; Beukelmann and Wier, 1988; McGuigan and Blatter, 1987). This procedure also requires that 1) there be negligible indicator bleaching during the confocal scan, 2) the indicator concentration be constant, and 3) the dye path length be constant. These requirements are met because the confocal microscope provides a cell section of constant thickness and, at the illumination power used, there was negligible bleaching during the scan. Movement artifacts were avoided by restricting calibration to the time before cell movement was detected or else by inhibiting contraction with BDM.

Use of line-scan images for studying $[Ca^{2+}]_i$ uniformity

A laser-scanning confocal microscope (LSCM) generates raster-scanned images by rapidly moving the focused laser beam over the cell, and it takes between 0.1 and 4.0 s to obtain an image, depending on the spatial resolution of the acquired image and the scan speed. This limited whole-cell image acquisition time precludes detailed examination of the rising phase of the $[Ca^{2+}]_i$ transient, as illustrated in Fig. 1. Fig. 1 *A* shows the transmitted light image of the cell obtained with the confocal microscope and Fig. 1 *B* shows a fluorescent image of the same cell loaded with fluo-3 and field stimulated when the scan was halfway through the cell. The increase in fluorescence of the cell is due to the increases in $[Ca^{2+}]_i$ evoked by the stimulus, but because each line in the image is separated by 2 ms, the image does not reflect a "snapshot" of the calcium distribution within the cell. Thus $[Ca^{2+}]_i$ is being measured at different times at different points within the cell, and it is not possible to extract the time course of change in $[Ca^{2+}]_i$ at any one point with such an image. To overcome this problem, the same line across the cell can be repeatedly scanned and the intensity of each scan line displayed as a "waterfall" plot by placing successive lines below each other (Fig. 1 *C*). With this approach, spatial information in one dimension is discarded to provide a higher time resolution (2 ms). Thus the horizontal dimension in the plot is distance along the scan line, whereas the vertical dimension is time (increasing from top to bottom). Note that the cell contraction is visible as a shortening of the fluorescent region and that the $[Ca^{2+}]_i$ transient clearly precedes the contraction.

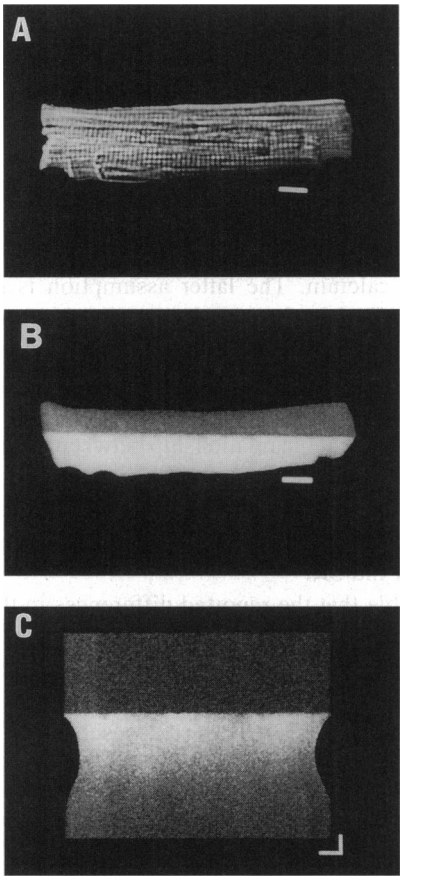

FIGURE 1 (*A*) Transmitted light micrograph of a single rat heart cell loaded with fluo-3. Scale bar 10 μm. (*B*) Fluorescence image of the cell shown in (*A*). The resting distribution of fluorescence was quite uniform and the cell was electrically stimulated when the confocal scan was halfway across the cell. Note the distortion of the ends of the cell as the cell contracts implying that the image is not a "snapshot" of the $[Ca^{2+}]_i$ distribution in the cell. Scale bar 10 μm. (*C*) Line-scan image of the same cell as in (*A*) and (*B*). This image was constructed by taking repeated scans along the same line and plotting the intensity of each scan line underneath each other. 456 ms after starting the line-scan image the cell was electrically stimulated. This resulted in a rapid increase in fluorescence along the scanned line, corresponding to an increase in $[Ca^{2+}]_i$. In addition, the cell contraction is visible as a shortening of the length of the scanned line. Note the high level of spatial and time resolution. Scale bar 10 μm horizontally, 100 ms vertically.

RESULTS

Imaging the $[Ca^{2+}]_i$ transient

A recent series of experiments using the LSCM have demonstrated that SR calcium release can be viewed at rest and during electrically activated calcium transients (Cheng et al., 1993). To a first approximation, these experiments showed that the stimulated calcium transients appeared to rise quite uniformly as a result of synchronized activation of SR calcium release. The experiments reported here were designed to extend these initial observations and examine, in detail, the uniformity of the SR calcium release activated by depolarization.

Close examination of the data shown in Fig. 1 *C* reveals some non-uniformity in the fluorescence signal. Another cell is shown in Fig. 2 *A* where the non-uniformity has been enhanced by increasing both the illumination intensity and the display contrast. The scan was started 456 ms before the cell was electrically stimulated, and the stimulus resulted in a rapid increase in fluorescence throughout the cell. After a short delay, the cell contracted by about 8.6%. It is notable that the increase in fluorescence did not occur as a sharp line across the cell, implying that calcium release was not spatially uniform, although there is no obvious systematic variation in the time course of calcium release. By averaging pixels in Fig. 2 *A* in the horizontal direction, the time course of the spatial averaged fluorescence can be determined, and the length of the scanned line provides a measure of the cell shortening. Fig. 2 *B* shows the time course of these measures taken from the line-scan image in Fig. 2 *A*. Approximately 4 ms after the electrical stimulus, the fluo-3 fluorescence starts to rise, reaching 90% of its final level in 36 ms and peaking at 48 ms. The cell contraction starts at 34 ms, reaching 90% of maximum in 94 ms and peaking at 112 ms. After reaching maximum, the fluorescence declines with a half time of 138 ms and contraction declines with a half time of 104 ms.

Because there is a delay before cell movement occurs, the spatial non-uniformities in the line-scan image of fluorescence changes cannot be explained by movement artifacts.

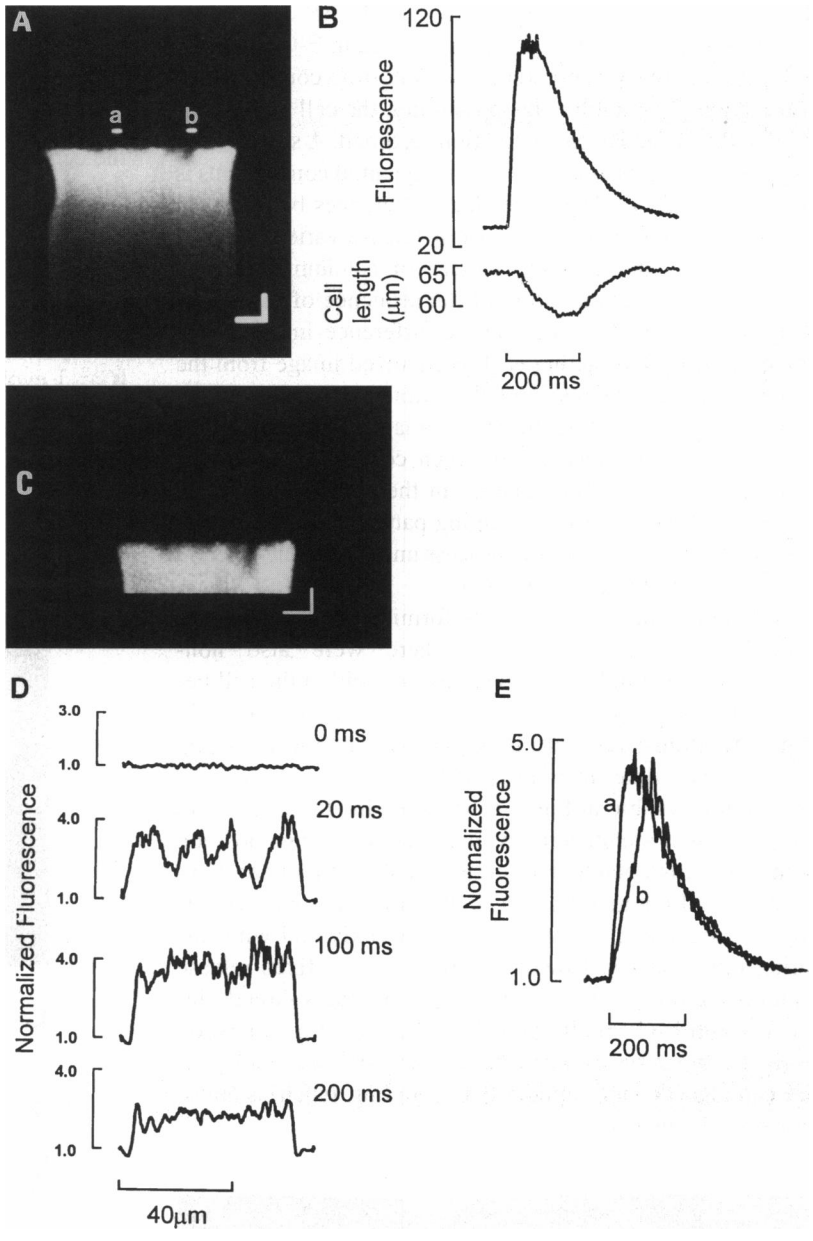

FIGURE 2 (*A*) Line-scan "waterfall plot" of an electrically evoked $[Ca^{2+}]_i$ transient. Note the non-uniformity in fluorescence visible as gaps in the otherwise steplike increase in fluorescence. The gaps occur before significant cell shortening occurs (visible as a reduction in the length of the scanned line). Scale bar 20 μm horizontal, 100 ms vertical. (*B*) The time course of spatial averaged fluo-3 fluorescence and cell contraction form the data in (*A*). Note the rapidity of the increase in fluorescence compared with contraction. (*C*) Expanded and normalized (see Materials and Methods) fluorescence record around the time of stimulation. Normalization did not remove the non-uniformity in the signal, and the non-uniformity appeared before cell contraction occurred. Scale bar 20 μm horizontal, 50 ms vertical. (*D*) Normalized fluorescence along scan lines at various times after stimulation. At rest the image is quite uniform, but 20 ms after stimulation the normalized fluorescence became very non-uniform. The uniformity of the normalized fluorescence signal then increases with time. (*E*) Time course of normalized fluorescence from the two regions indicated in (*A*). The indicated regions were 5.8 μm wide. Note the slow increase in fluorescence in region *b* as compared with region *a*. However, the time course of the signal from the two regions becomes very similar after the peak of the $[Ca^{2+}]_i$ transient.

The non-uniformities in the fluorescence signal are shown at higher resolution in Fig. 2 *C*, in which the data has been normalized (see Materials and Methods) to remove possible non-uniformities in dye distribution. The local variations in the time course of the fluorescence change were largely unaltered by the normalization procedure, from which we conclude that the resting distribution of fluo-3 cannot explain such large variations in the time course of rise in $[Ca^{2+}]_i$. Fig. 2 *D* shows the normalized fluorescence profile along single scan lines just before stimulation (0 ms), and then at 20, 100, and 200 ms after stimulation. It is clear that the spatial non-uniformity is largest during the rise of the $[Ca^{2+}]_i$ transient and that the non-uniformity largely disappears during the falling phase of the $[Ca^{2+}]_i$ transient. To quantify the time course of the change in $[Ca^{2+}]_i$ at two different regions within the cell, the intensity (of the regions shown as bars in Fig. 2 *A*) is plotted against time in Fig. 2 *E*. The fluorescence ratio of the region on the right rises more slowly than the region on the left, but the signal from both regions decays with a similar time course. The fact that the traces merge during the relaxation phase of the transient supports the idea that these spatial non-uniformities in fluorescence are not due to differing dye distributions or movement artifacts. We therefore conclude that there are significant spatial non-uniformities in $[Ca^{2+}]_i$ that develop during the early part of the electrically evoked calcium transient, and these non-uniformities dissipate during the relaxation phase of the $[Ca^{2+}]_i$ transient.

Beat to beat variation in $[Ca^{2+}]_i$

If the observed variations in the spatial distribution of $[Ca^{2+}]_i$ during the upstroke of the $[Ca^{2+}]_i$ transient were due to

differences in the spatial organization of the SR or the presence of sub-cellular structures not involved in E-C coupling, the pattern of release should be constant, from contraction to contraction. To examine this possibility, the cell was stimulated at 0.5 Hz and each contraction recorded. A sequence of five line-scan plots associated with sequential contractions is shown in Fig. 3 *A*. There are clear differences between the images, showing that the pattern of release varied between contractions. The changing pattern of calcium release is made clearer on examination of the sequence of difference images shown in Fig. 3 *B*. These difference images were constructed by subtracting each normalized image from the preceding image and rescaling the output between black and white. The four resulting difference images show the pattern of calcium release changes between contractions and that there are not systematic changes in the pattern of calcium release. The nature of the changing patterns of release suggests that there is a stochastic process underlying the calcium release evoked by depolarization.

Although some of the non-uniformities in $[Ca^{2+}]_i$ were variable between contractions, there were also non-uniformities that did not change position within the cell between stimuli. This point is illustrated in Fig. 3 *C*, where 20 stimulated transients were averaged. Given that averaging will preserve time-invariant patterns of release, the non-uniformities visible in Fig. 3 *C* are more likely to be due to the subcellular architecture, which does not change position with time. It is notable that these data show that $[Ca^{2+}]_i$ increases at all points within the cell; however, some regions appear to respond, on average, more weakly and with differing time courses. However, whether these fixed release patterns are due to the distribution of structures directly involved with E-C coupling (such as the spatial organization of the t-tubular system) or whether they are due to areas of the cell that do not support E-C coupling (such as mitochondria) is unclear.

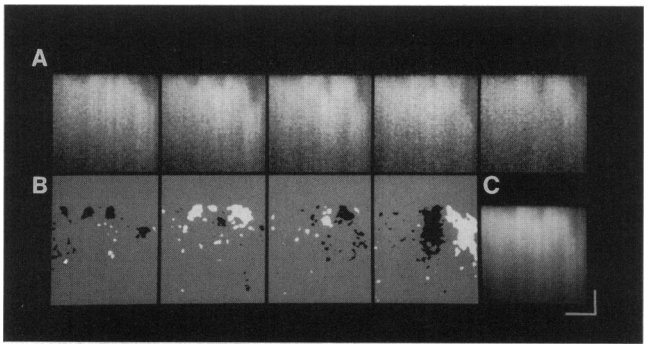

FIGURE 3 (*A*) The top series of panels shows five sequential line-scan images. Note the varying pattern in the normalized fluorescence record just after the point of stimulation (near the rapid increase in signal associated with the upstroke of the $[Ca^{2+}]_i$ transient). (*B*) A sequence of difference images from the data shown in (*A*). A threshold has been applied to the data to clarify differences between pairs of images. (*C*) Averaged line-scan image from the data shown in (*A*). Note that some of the non-uniformity in normalized fluorescence is relatively time invariant as shown by the persistence of patterns in this averaged image. Scale bar 10 μm horizontally, 100 ms vertically.

Uniformity of sarcolemmal calcium influx

In principle, the non-uniformities in $[Ca^{2+}]_i$ could arise either from non-uniformities in calcium release from the SR or from alterations in the distribution of calcium current across the cell. Given that the calcium current provides the trigger for calcium release from the SR, non-uniformities in calcium current could be amplified by calcium release from the SR. To examine this possibility, SR calcium metabolism was inhibited with ryanodine (McPherson and Campbell, 1993) and thapsigargin (Kirby et al., 1992) (to block SR calcium release and uptake, respectively). In these conditions the increase in $[Ca^{2+}]_i$ evoked by depolarization was much smaller, and the consequent reduction in the signal-to-noise ratio prevented detailed examination of the distribution of the rise in $[Ca^{2+}]_i$. To ameliorate this effect partially the calcium concentration in the bathing solution was increased to 10 mM. Fig. 4 shows

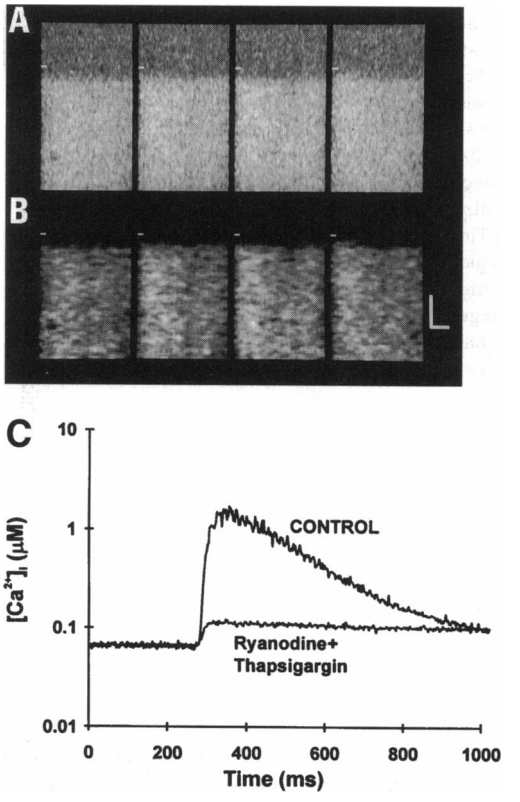

FIGURE 4 Normalized fluorescence transients in the presence of SR inhibitors (1 μM ryanodine to block SR release channels and 1 μM thapsigargin to block SR calcium uptake). The bathing calcium was raised to 10 mM to increase the amplitude of the $[Ca^{2+}]_i$ transient in the these conditions. The time of stimulation is indicated by a small horizontal bar at the left of each panel. Note that, despite the reduction in signal (and signal-to-noise ratio) the increase in $[Ca^{2+}]_i$ still occurred rapidly across the width of the region scanned. (*B*) To accentuate any non-uniformities in $[Ca^{2+}]_i$, the images in (*A*) were filtered (filter half-widths 1.0 μm and 6 ms) and the contrast stretched. Some non-uniformity in the time of rise of the signal after stimulation can be seen in these images. Scale bar 5 μm horizontal, 50 ms vertical. (*C*) The normalized fluorescence signal in control conditions and after exposure to ryanodine and thapsigargin was converted to $[Ca^{2+}]_i$ as detailed in Materials and Methods. Note that $[Ca^{2+}]_i$ is plotted on a logarithmic scale and that ryanodine and thapsigargin profoundly depressed the amplitude of the $[Ca^{2+}]_i$ transient while slowing its decay.

a series of line-scan images of the rise in $[Ca^{2+}]_i$ evoked by depolarization in these conditions. Although there is noise in the data, a couple of features are notable. 1) The rise in $[Ca^{2+}]_i$ occurs across the whole cell with little delay, showing that there must be calcium channels in the t-tubular system. 2) Although weak, there are some non-uniformities in $[Ca^{2+}]_i$ that are variable between images. To clarify the latter point, the images were low-pass filtered to give a spatial resolution of 1.0 μm, and the contrast increased (Fig. 4 *B*). After this image processing, the differences between the images are clearer. Thus, although noisy, these data suggest there is some spatial non-uniformity in the calcium current (and other sources for calcium influx; see Discussion). Nevertheless, the rise in $[Ca^{2+}]_i$ due to the calcium current occurs virtually simultaneously at the sarcolemmal surface and deep within the cell, as would be required to support synchronized CICR throughout the cell.

The time course of the $[Ca^{2+}]_i$ transient calculated from the normalized fluorescence record is shown in Fig. 4 *C* as well as the $[Ca^{2+}]_i$ transient observed before exposure to ryanodine and thapsigargin. The large decrease in the amplitude of the $[Ca^{2+}]_i$ transient is expected from previous work supporting the idea that the calcium current supplies only a small fraction of the calcium required for normal contraction (Cannell et al., 1987b; Sipido and Wier, 1991; Kirby et al., 1992; Varro et al., 1993). In addition, the declining phase of the $[Ca^{2+}]_i$ transient was slowed, demonstrating the importance of SR calcium uptake in the decline of the calcium transient (Cannell, 1991; Kirby et al., 1992; Bers et al., 1989). An estimate of the relative contribution of the calcium current to the $[Ca^{2+}]_i$ transient can be made by comparing the relative amplitudes of the transients shown in Fig. 4 *C*. In eight similar experiments (where the bathing calcium concentration was kept constant at 1 mM), the amplitude of the $[Ca^{2+}]_i$ transient in control conditions was 1.57 ± 0.1 μM, which decreased to 34 ± 10.7 nM in the presence of ryanodine and thapsigargin. Thus the sarcolemmal trigger calcium appeared to provide ~2.2% of the total calcium influx (with the first-order assumption that the change in peak $[Ca^{2+}]_i$ is proportional to the influx).

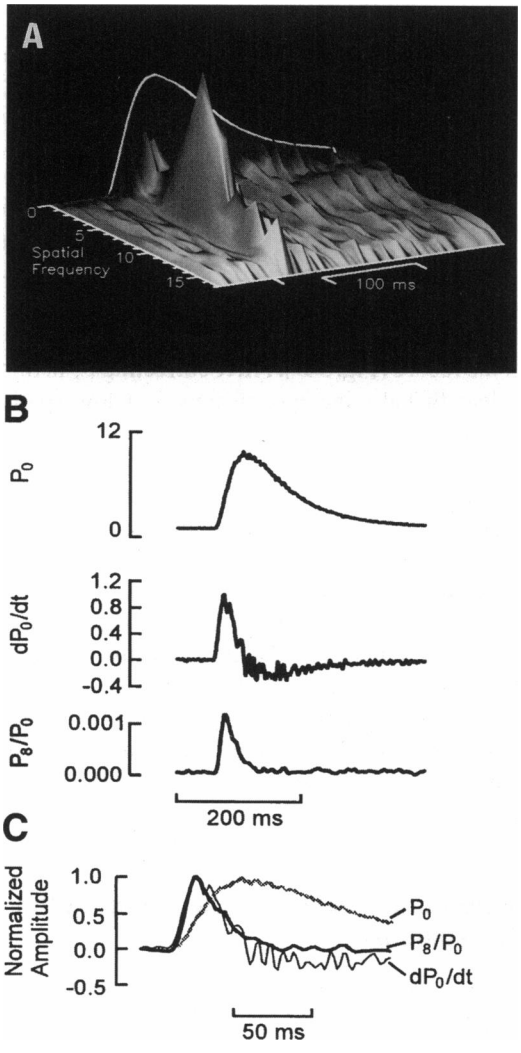

FIGURE 5 (*A*) Power spectra of lines scanned during an electrically evoked $[Ca^{2+}]_i$ transient. The spatial frequency is calibrated in cycles per 100 μm, and the time of stimulation is marked by a tick mark on the time axis. The time course of the amplitude of the normalized fluorescence transient is shown at the "back" of the plot (edged in white). Note the burst of low-frequency power associated only with the rising phase of the $[Ca^{2+}]_i$ transient. (*B*) Time course records showing (top to bottom) amplitude of the normalized fluorescence transient (extracted from the 0 spatial frequency component), the time derivative of the normalized fluorescence transient and excess power in the eight cycles/line spatial frequency range during the $[Ca^{2+}]_i$ transient. (*C*) Comparison of the time course of the records shown in (*B*). Note the similarity in the time course of the derivative and the low-frequency power components, and that these components declined to low levels by the time the peak of the $[Ca^{2+}]_i$ transient occurred.

Time course of the spatial non-uniformity

As noted earlier, the observed non-uniformities in $[Ca^{2+}]_i$ were most prominent during the early part of the $[Ca^{2+}]_i$ transient. To obtain a more quantitative measure of the time course of non-uniformities in $[Ca^{2+}]_i$, power spectra of the line-scan data were calculated. The Fourier transform of each scanned line was calculated and the low-frequency components in the power spectrum displayed in a shaded surface plot (Fig. 5 *A*) to show the variation in the power spectra with time during the $[Ca^{2+}]_i$ transient. There was a marked increase in power at low spatial frequencies during the rising phase of the $[Ca^{2+}]_i$ transient, but the time course of this increase in power was of shorter duration than the calcium transient. The increase in the amplitude of the low spatial frequency components was therefore due to spatial non-uniformities in $[Ca^{2+}]_i$ at early times during the $[Ca^{2+}]_i$ transient. It should be noted that the appearance of these low-frequency components is not explainable by photon noise in the line-scan images because 1) the shot noise spectrum extends uniformly across all frequencies so that 2) the time course of the amplitude of the shot noise spectrum should be the same as the time course of fluorescence change.

The "burst" of low-frequency power occurred in the spatial frequency domain of 6–18 cycles/line-scan line (which was 100 μm long) and was of shorter duration than the

$[Ca^{2+}]_i$ transient. To examine the time course of the development and decay of the low-frequency components (i.e., spatial non-uniformity in $[Ca^{2+}]_i$), the amplitude of the most prominent component (at 8 cycles/line, P_8) was divided by the amplitude of the fluorescence signal (which was the component of the power spectrum at 0 spatial frequency, P_0). Given that the photon noise (shot noise) power spectrum extends across all spatial frequencies and has a density dependent on the amplitude of the fluorescence signal, dividing the spectral components by the fluorescence amplitude should suppress signal components arising from photon noise in the record (Fig. 5 *B*). After correcting P_8 in this way, it was clear that the increase in power at low spatial frequencies (P_8/P_0) was of much shorter duration than the $[Ca^{2+}]_i$ transient.

To a first approximation, the time derivative of the $[Ca^{2+}]_i$ transient is proportional to the rate of calcium release into the cell (Melzer et al., 1987; Sipido and Wier, 1991). The time course of development and decay of the low-frequency components and the derivative of the fluorescence signal (Fig. 5 *C*) were very similar, except that the derivative became negative after the peak of the $[Ca^{2+}]_i$ transient. The similarities in the time course of the derivative signal and the power signal supports the idea that the observed spatial non-uniformity in $[Ca^{2+}]_i$ arises from the time course of calcium release within the cell.

Spatial non-uniformities in $[Ca^{2+}]_i$ during the negative staircase

If the non-uniformities of $[Ca^{2+}]_i$ are due to weaker E-C coupling in some regions of the cell, then the apparent gain of the CICR mechanism could be a major factor in determining which regions release calcium. It has been proposed that the gain of CICR may be dependent on the SR lumen calcium level (Niggli and Lederer, 1990a; Cheng et al., 1993), so that interventions that alter the SR calcium content may alter the pattern of calcium release. Because a decrease in contraction strength during negative staircases may be due to a decrease in the calcium content of the SR (duBell et al, 1993; Bouchard and Bose 1992; but see Bouchard and Bose, 1989), it was of interest to examine whether the decrease in contraction strength was associated with an alteration in the number of regions that release calcium. To examine this point, 2,3-butanedione monoxime (BDM) was added to the bathing medium to minimize cell contraction and prevent possible movement artifacts. It has been previously shown that BDM does not block the intracellular $[Ca^{2+}]_i$ transient while profoundly depressing tension production (Li et al., 1985; Blanchard et al., 1990; Gwamathey et al., 1991; Györke et al., 1993; Steele and Smith, 1993).

Fig. 6. shows a series of four stimuli from the rested state and, as shown earlier, non-uniformities in $[Ca^{2+}]_i$ were observed after each stimulus. In the panels below each waterfall plot the time courses of normalized fluorescence, and low spatial frequency power are shown (Fig. 6 *B*). With successive contractions, the amplitude of the $[Ca^{2+}]_i$ transient decreased, but the time course of SR release and the time course of the development and decay of spatial non-uniformity in $[Ca^{2+}]_i$ were relatively constant. Given that the relative extent of spatial non-uniformity was approximately constant, the 70% decrease in the amplitude $[Ca^{2+}]_i$ transient during the negative staircase is more likely to be due to a decrease in the amount released at each site within the cell than to a decrease in the number of sites that release calcium.

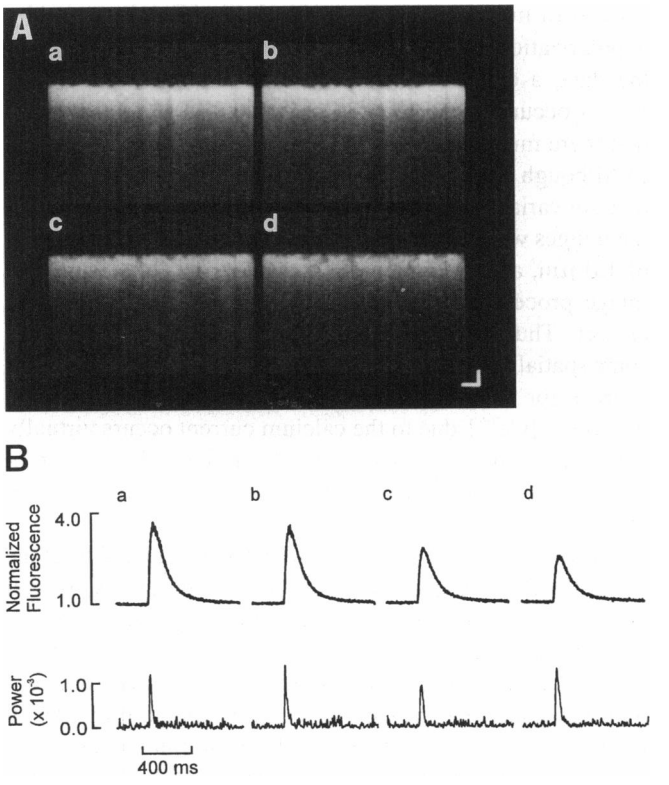

FIGURE 6 (*A*) Line-scan images (normalized) during the first four beats of the negative staircase. Note the non-uniformity at the rising edge of the $[Ca^{2+}]_i$ transient. Scale bar: 10 μm horizontal, 100 ms. (*B*) Time course of normalized fluorescence amplitude and excess low frequency power associated with the four contractions shown in (*A*). Although the fluorescence decreases during the staircase, the peak power in each trace is comparable.

Reducing sarcolemmal calcium current increases spatial non-uniformity of $[Ca^{2+}]_i$

The amplitude of the $[Ca^{2+}]_i$ transient is also modulated by the amplitude of the calcium current (Cannell et al., 1987b; Barcenas-Ruiz and Wier, 1987; duBell and Houser, 1989; Callewaert et al., 1988). As noted above, modulation of the amplitude of the $[Ca^{2+}]_i$ transient could be due either to an alteration in the amount released at each site or to an alteration in the number of sites that release calcium (or both). To examine the relationship between the calcium current and $[Ca^{2+}]_i$ non-uniformities, the calcium current was inhibited with a low concentration of Cd^{2+}. Fig. 7 *A* shows a line-scan image of the evoked $[Ca^{2+}]_i$ transient obtained from the rested state in the presence of 10 μM Cd^{2+}. The gross non-uniformity of $[Ca^{2+}]_i$ observed in these conditions appeared

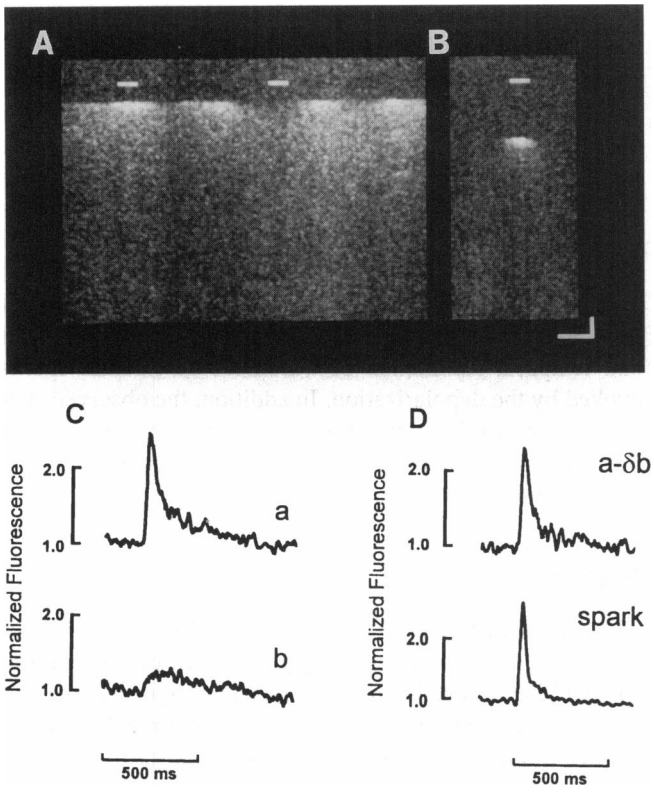

FIGURE 7 Spatial non-uniformity in the presence of Cd^{2+}. (*A*) After exposure to 10 μM Cd^{2+}, the evoked $[Ca^{2+}]_i$ transient appears to occur in only a limited number of regions. These evoked increases in $[Ca^{2+}]_i$ had a marked similarity to spontaneous calcium sparks (*B*). (*C*) The time course of the normalized fluorescence from the two regions indicated in (*A*) are shown as traces *a* and *b* (from the left and center regions of (*A*), respectively). Note the low amplitude of the $[Ca^{2+}]_i$ transient in these conditions (compare Figs. 2 *E* and 6 *B*). (*D*) To extract the time course of fluorescence change at the sites that released calcium, the difference between trace *a* (of (*C*)) and the change in fluorescence in regions (along the same scan line) that did not release calcium (δb) is plotted in the top trace. The time course of fluorescence change evoked by depolarization in the presence of Cd^{2+} is very similar to spontaneous calcium sparks, both in amplitude and time course. Scale bars: 5 μm and 100 ms.

to arise from a limited number of discrete sites that released calcium. It was suggested earlier (Cheng et al., 1993) that the calcium spark is an elementary event underlying E-C coupling, in which case the data in Fig. 7 *A* could be explained by calcium release being reduced to the point where only a few calcium sparks are evoked by the depolarization. This view is supported by comparing the pattern of calcium release in the presence of Cd^{2+} to a typical spontaneous calcium spark (Fig. 7 *B*). Visual comparison of *A* and *B* of Fig. 7 suggests that the pattern of release in the presence of Cd^{2+} was very similar to a limited number of calcium sparks, except that the calcium sparks were synchronized to the depolarizing pulse instead of occurring spontaneously.

This view is supported by comparing the time course and amplitude of the changes in normalized fluorescence of the regions shown in Fig. 7, *A* and *B*. Fig. 7 *C* shows the time course of normalized fluorescence at the site of an evoked spark (trace *a*) and at a region between the sparking sites (trace *b*). The small, slow increase in $[Ca^{2+}]_i$ seen in trace *b* probably reflects the diffusion of calcium from sites of release both within and outside the confocal plane. To compare the amplitude and time course of these evoked local increases in $[Ca^{2+}]_i$ with calcium sparks the increase in $[Ca^{2+}]_i$ due to diffusion from sites outside the focal plane was subtracted from trace *a* (Fig. 7 *D*). It is clear that the amplitude and time course of the increase in $[Ca^{2+}]_i$ at the local sites that are observed in the presence of Cd are very similar to a spontaneous calcium spark. We therefore conclude that under these conditions, E-C coupling takes place in the form of a limited number of calcium sparks that are triggered by the depolarization.

Imaging calcium release sites during normal E-C coupling

The data presented above suggested that calcium release during E-C coupling was the result of the summation of a finite number of calcium sparks, at least when the calcium current was inhibited with Cd^{2+}. To examine the extent to which the normal calcium transient can be explained by the summation of a larger number of evoked calcium sparks, images showing spatial non-uniformity of the type shown above were analyzed with an deconvolution procedure (see Fig. 8).

The first stage of the deconvolution algorithm assumed that calcium sparks such as those shown in Fig. 7 *B* were present in the calcium transient and calculated how many calcium sparks would be needed to give the spatially averaged signal on each scan line (N_t), while also taking into

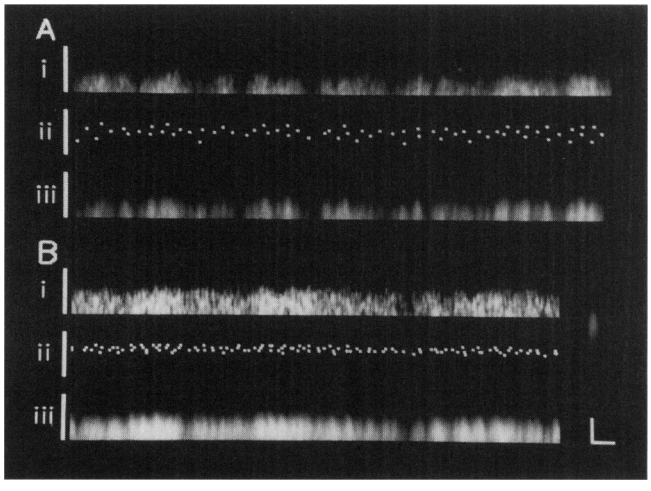

FIGURE 8 Summation of calcium sparks evoked by depolarization can explain the $[Ca^{2+}]_i$ transient non-uniformity. Figs. *Ai* and *Bi* show normalized line-scan image data from the first 28 ms of an evoked $[Ca^{2+}]_i$ transient from two different cells. For both cells, the calculated position and timing of calcium spark occurrence during the evoked transient are shown in the panels marked *ii*. Note that the spark site density is unevenly distributed, with some sites initiating calcium sparks after a delay. The spontaneous calcium spark that was used in processing the original data is shown on the right. In the panels marked *iii*, the non-uniformity in the rising phase of the $[Ca^{2+}]_i$ transient is reconstructed from the spark site data. Scale bar 5 μm horizontally, 20 ms vertically.

account the time varying contribution of sparks on previous scan lines:

$$N_o = \frac{\int_x F_o}{\int_x S_o}; \qquad N_t = \frac{\int_x F_t - \sum_{j=0}^{j=t-1} \left(N_j \int_x S_{(t-j)} \right)}{\int_x S_o} \tag{4}$$

where S_t is the fluorescence in a spark image (shown in Fig. 8) on scan line t; F_t is the fluorescence in the image at scan line t and x the spatial coordinate).

Next, a cross-correlation (R_n) between a typical calcium spark ($S(y, t)$) and the line-scan fluorescence image (F_n) where the nth spark occurred. The maximum of this correlation gave the spatial coordinate of the nth spark (X_n).

$$\left\{ \begin{array}{l} R_n(x) = \iint_{y,t} S(y, t) F_n(x + y, t + T_n)\, dy\, dt \\ \\ X_n : R_n(X_n) = \max(R_n(x)) \end{array} \right\} \tag{5}$$

where

$$\left\{ \begin{array}{l} F_1 = F \\ F_n = F_{n-1} - S(x + X_{n-1}, t + T_{n-1}) \end{array} \right\} \tag{6}$$

In other words, the original fluorescent images (Fig. 8, *Ai* and *Bi*) were used only for deriving the position of the first spark site. Modified images (F_n) were then constructed by subtracting the contribution of previously located sparks from them, which were then used in the cross-correlation. (Because the algorithm was iterative, the subtraction of sparks prevented the algorithm from continuously placing sparks at the same location.) The subtraction and cross-correlation steps were repeated until N_t sparks had been located on each scan line. These steps of the algorithm therefore gave an output image (Fig. 8, *Aii* and *Bii*) that represented the coordinates (position and timing) of calcium sparks that would be required to give the observed line-scan fluorescence image. Finally, the timing and position data were used to reconstruct the original image (Fig. 8, *Aiii*, *Biii*) by convolving the coordinate data (image) with a calcium spark to allow visual comparison with the original data.

As shown in Fig. 8 *A*, this algorithm was applied to the rising phase of a calcium transient recorded from a cell whose spatial averaged transient was associated with a peak fluorescence ratio of 3.2 (occurring 30 ms after stimulation). The original image is shown in Fig. 8 *Ai*, and the output image (showing the calculated coordinates of the spark sites) is shown in Fig. 8 *Aii*. The result of the convolution of the calcium spark with the output image is shown in Fig. 8 *Aiii*, and it is apparent that the spatial non-uniformity observed in the original image is very similar to that seen in the convolved image. Thus the spatial non-uniformity in this cell can be explained by the activation of calcium sparks at various times and positions after the stimulus. In another cell (Fig. 8 *B*), in which E-C coupling was more potentiated (as evidenced by a peak fluorescence ratio of 3.9 occurring 12 ms after stimulation, which would correspond to $[Ca^{2+}]_i \approx 1.42\mu$ M as compared with $[Ca^{2+}]_i \approx 0.71\ \mu$M in cell A) the algorithm predicted that the calcium sparks occurred more rapidly after stimulation with a density of 1.15 sparks/μm. The time course of the change in calcium spark density was bell-shaped with a peak spark density occurring at 10 and 8 ms after stimulation, and was complete within 20 and 12 ms (cells A and B, respectively). These data therefore show that the normal $[Ca^{2+}]_i$ transient can be explained by the spatial and temporal summation of a number of calcium sparks evoked by the depolarization. In addition, the observed spatial non-uniformity in the $[Ca^{2+}]_i$ transient is consistent with the presence of calcium sparks whose occurrence is a time-dependent stochastic process.

DISCUSSION

The data presented here show that spatial non-uniformities in $[Ca^{2+}]_i$ occur during the rising phase of the depolarization-evoked $[Ca^{2+}]_i$ transient in rat ventricular myocytes. Analysis of these non-uniformities, as well as experiments in which E-C coupling is modified by drugs, suggests that a large component of these non-uniformities is due to the stochastic activation of SR Ca-release channels. The stochastic quantal nature of E-C coupling reported here supports the idea that the calcium spark (Cheng et al., 1993) is an elementary event that underlies normal E-C coupling. It then follows that graded calcium release will arise from alterations in the time course of calcium spark activation (an inherently stochastic process) as well as possible modulation of their amplitude by changes in the SR luminal calcium concentration.

Detection of spatial non-uniformity in $[Ca^{2+}]_i$

The results presented here show that the LSCM can detect spatial non-uniformities in $[Ca^{2+}]_i$ that develop during the rising phase of the calcium transient. Previous imaging studies (e.g., Cannell et al., 1987a, Berlin et al., 1989 Takamatsu and Wier, 1990a,b) did not resolve these non-uniformities, probably because the conventional (wide-field) fluorescence microscope suffers from a loss of contrast as a result of out-of-focus fluorescence. In addition, the most prominent non-uniformities in $[Ca^{2+}]_i$ last only about 10 ms, which is less than the conventional video image acquisition time (~30 ms). Furthermore, the fluorescence of fluo-3 is low at resting levels of $[Ca^{2+}]_i$ (Minta et al., 1989), so that the contrast of the images presented here is considerably greater than those obtained previously with other fluorescent indicators. Although it was possible to detect spatial non-uniformity in $[Ca^{2+}]_i$ between regions separated by only a few μm, the detection of the predicted gradients in $[Ca^{2+}]_i$ at the subsarcomeric level (see Cannell and Allen, 1984; Wier and Yue, 1986) appears to be beyond the resolution of the LSCM at this time. This is because the volumes involved are too small, and therefore do not contain enough fluorescent indicator, to

obtain usable signals at the temporal resolution needed (<10 ms) to resolve such subsarcomeric gradients.

Patterns in fluorescence non-uniformity

After normalizing the fluorescence image, there were non-uniformities in the evoked $[Ca^{2+}]_i$ transient. Two components in the spatial non-uniformity in $[Ca^{2+}]_i$ were detected. One component was time invariant; this component can be most simply explained by the presence of subcellular structures (such as mitochondria) that are not directly involved in E-C coupling, as well as the organization of the t-tubules and junctional SR. A second kind of spatial non-uniformity of $[Ca^{2+}]_i$ has already been reported by Niggli and Lederer (1990b), who found that during a stimulated $[Ca^{2+}]_i$ transient, fluo-3 fluorescence increases in the nucleus, but this increase was delayed as calcium diffused into the nucleus from the cytosol. We avoided this kind of spatial non-uniformity of $[Ca^{2+}]_i$ by obtaining optical sections that did not include the nucleus.

Secondly, there were non-uniformities in $[Ca^{2+}]_i$ that varied in position between stimuli, and which probably reflect changing patterns of $[Ca^{2+}]_i$ release. The presence of subcellular structures cannot explain the varying patterns of $[Ca^{2+}]_i$ release, because the position of subcellular structures should be time invariant. In addition, movement of the cell with respect to the confocal plane cannot explain the varying patterns of calcium release, given that non-uniformities are detectable before cell movement starts (as indicated by movement of the edge of the cell) and when the cell was treated with BDM, a potent inhibitor of cell contraction.

It is also notable that the depolarization-evoked $[Ca^{2+}]_i$ transient became increasingly uniform as the peak of the transient was approached. This result suggests that calcium must diffuse readily within the cytosol from the sites of release and that the sites of calcium release are sufficiently close together to ensure that large gradients of $[Ca^{2+}]_i$ are dissipated by the time the peak of the $[Ca^{2+}]_i$ transient is reached. The rapid dissipation of $[Ca^{2+}]_i$ gradients helps explain why previous studies did not resolve the non-uniformities in $[Ca^{2+}]_i$ reported here (see above). In addition, this result supports the idea that the non-uniformities seen at early times during the $[Ca^{2+}]_i$ transient are not due to the physical exclusion of calcium from regions of the cell.

Time course of E-C coupling across the cell

Apart from the local stochastic non-uniformities in $[Ca^{2+}]_i$ described above, the experiments showed that E-C coupling takes place virtually synchronously throughout the cell. The lack of detectable difference in the time of rise of $[Ca^{2+}]_i$ between the center and the edge of the cell (so the rise in $[Ca^{2+}]_i$ appears almost as a step in the line-scan images) suggests that the trigger for CICR is a local increase in $[Ca^{2+}]_i$ rather than the diffusion of calcium from the surface membrane to the center of the cell. Given that the L-type calcium current is generally thought to supply the trigger calcium for E-C coupling, we are forced to conclude that functional L-type calcium channels must exist in the t-tubular system. This view is supported by the observation that 10 μM Cd^{2+} dramatically alters the pattern of $[Ca^{2+}]_i$ release across the cell. In addition, exposure of the cell to SR inhibitors results in smaller transient that also appears as a step in the line-scan image (Fig. 4). It seems likely that the rise of $[Ca^{2+}]_i$ in these conditions is due to the activation of L-type calcium channels by the rapid propagation of the action potential into the center of the cell. Whereas the existence of L-type calcium channels (which activate calcium release by CICR) in the t-tubular membrane has been assumed by the majority of workers when discussing E-C coupling (e.g., Callewaert, 1992; Bers and Stiffel, 1993), the data presented here directly demonstrate that the trigger calcium influx occurs via Cd^{2+}-sensitive (L-type) calcium channels throughout the t-tubular system.

Relationship between non-uniformity in $[Ca^{2+}]_i$ and E-C coupling

Non-uniformities in $[Ca^{2+}]_i$ that vary between contractions can be explained by two different mechanisms: 1) alterations in the amount of calcium available for release in the SR, and 2) changes in the number of SR release channels that open on depolarization.

During steady-state contractions, it is likely that the amount of calcium in each element of the SR would be relatively constant, as regions that had a low calcium content would become replenished at the expense of other regions with a higher calcium content. As shown in Fig. 2, $[Ca^{2+}]_i$ becomes more spatially uniform during the relaxation phase of the $[Ca^{2+}]_i$ transient, so that by the end of relaxation each SR element would contain an amount of calcium that would depend principally on the ability of that element to take up calcium. Although we cannot exclude a possible beat-to-beat modulation of the ability of the SR elements to take up calcium, it seems likely that SR calcium uptake (and hence SR calcium content) should be relatively constant in the steady state.

The second possibility, that there are variations in the number of SR release channels that open with each depolarization, seems a more likely candidate for the source of the spatial variation in $[Ca^{2+}]_i$. Indeed, stochastic variation in the number of open channels is expected, and the effects of such variation become effectively larger as the number of channels decreases. In view of the proposed role of the L-type calcium channel in triggering CICR, stochastic variation in the number of open SL calcium channels would affect the number of SR release channels that open. Furthermore, even if "activated" the intrinsic gating of the SR release channels will contribute to variations in calcium release. Given that the rat heart cell contains about 150 fmol dihydropyridine receptor (DHPR) binding sites per mg protein and assuming 100 mg protein/cm^3 and a 1:1 relationship between DHPR and functional L-type calcium channels (Lew et al., 1991),

we can estimate that there should be about nine L-type calcium channels/μm^3. However, a recent electrophysiological study in guinea pig has suggested a density of 1.7 L-type channels/μm^2 (Rose et al., 1992). Given the relationship between t-tubular membrane area and cell volume (0.12 $\mu m^2/\mu m^3$ (Stewart and Page, 1978)), a much lower density of 0.2 channels/μm^3 is calculated. Such a low density does not seem compatible with the uniformity of the $[Ca^{2+}]_i$ transient observed in the presence of SR inhibitors (Fig. 4, and see below), and is also difficult to reconcile with the idea that the calcium current activates CICR in every sarcomere. It is possible that the recording conditions used by Rose et al. (1992) (i.e., the choice of holding potential and inhibition of Na/Ca exchange leading to an increase in $[Ca^{2+}]_i$) may have resulted in an erroneously low channel density. On the other hand, uncertainties in the stoichiometry of dihydropryridine binding may have led to an overestimate of the L-type calcium channel density. We therefore suggest that four channels/μm^3 may be closer to the actual L-type calcium channel density.

In rat ventricular cells, there are about seven times as many ryanodine receptors (RyR) as DHPR (Bers and Stiffel, 1993; Wilbo and Godfraind, 1991). However, the corbular SR is similar in morphology to the junctional SR and also contains RyR (Jorgensen et al., 1993). In rat, about 40% of the calsequestrin-containing SR is corbular (Jorgensen et al., 1985) and, assuming that the RyR is also evenly distributed in corbular SR, these considerations suggest a stoichiometry of 1 DHPR:4 junctional RyR:3 corbular RyR. To provide tight control of the RyR by the DHPR, the DHPR might lie opposite the center of a square formed by the four RyR at its corners. This possible arrangement would then represent the functional unit for depolarization-induced calcium release. Unfortunately, it is unclear whether the DHPR are confined to the junctional regions of the t-tubule, so it is also possible that more than four RyR may be controlled by each DHPR, as suggested by Bers and Stiffel (1993).

Despite the above uncertainty, the data presented here suggests that E-C coupling during the normal calcium transient can be explained by the presence of about 1.15 calcium sparks/μm along the scan line. As pointed out by Cheng et al. (1993), the calcium spark could reflect the flux of calcium from a small number of RyR acting in concert, and with functional units (as described above) containing a small number of RyR such concerted behavior is expected (Stern, 1992). Thus a functional unit would behave as if it were a single channel whose gating is modified by the calcium influx via a DHPR.

It has been estimated that the open probability (p_o) of an L-type channel may be 0.03 during depolarization (Lew et al., 1991; Rose et al., 1992) so that with four DHPR/μm^3 we might expect only one open channel every 8 μm along a confocal scan line. However, the activation of the $[Ca^{2+}]_i$ transient was considerably more uniform than this. It is possible to reconcile a more uniform level of activation with such a low p_o by considering the kinetics of calcium channel gating. Given that

$$p_o = \frac{t_{open}}{t_{open} + t_{closed}} \quad (7)$$

(where t_{open} and t_{closed} are the mean open and closed times respectively) a low p_o indicates $t_{open} \ll t_{closed}$. To achieve the activation of 1.15 spark/μm in the first 8 ms of E-C coupling, the average rate of spark production would have to be 144 $s^{-1}\mu m^{-1}$. Assuming that the opening of a single L-type calcium channel activates a spark (see below), and that there are four channels/μm along the scan line the mean opening rate of the L-type calcium channel ($1/t_{closed}$) would have to be >36 s^{-1}. This constraint would suggest that $t_{open} < 0.8$ ms, a comparable figure to that observed in single L-type calcium channel records (e.g., Rose et al., 1992). It is interesting to note that this model suggests that each functional release unit is activated only once by a brief opening of the L-type calcium channel during the rise of the $[Ca^{2+}]_i$ transient. This arises because the mean closed time would be about 27 ms, which is longer than the time course of calcium release. In connection with this point, if the calcium spark is activated by the first opening of a calcium channel, then the time course of calcium spark occurrence should be defined by the L-type latency for first opening probability density function. Fig. 8 shows that calcium spark occurrence reaches a peak ~9 ms after stimulation and is essentially complete by 20 ms. These figures are in good agreement with the L-type channel first-latency probability density function calculated by Rose et al. (1992), supporting the idea that activation of a functional SR calcium release is very tightly coupled to the opening of a single L-type calcium channel. The amplification of the trigger calcium by the release from the SR is therefore due to both the higher calcium flux through the open RyR functional units as well as the increased open time of the functional unit (which will be greater than the mean open time of an isolated RyR due to the clustering of RyRs in the functional unit; see Stern, 1992). Within this model, the L-type calcium channels density ensures that calcium release from the SR takes place rapidly despite the low p_o.

Interventions that reduce p_o of the L-type calcium will therefore reduce the spatial uniformity of $[Ca^{2+}]_i$ because the calcium release from each functional SR element will be under the local control of the calcium influx via its associated L-type calcium channel. This local control of the calcium release from the SR elements also predicts and explains the observed variation in the spatial uniformity of $[Ca^{2+}]_i$ during the rising phase of the $[Ca^{2+}]_i$ transient, given that the stochastic nature of the L-type calcium channel opening will lead to stochastic variation in the timing of SR release (spark activation).

Effect of partial Ca-channel blockade

Low concentrations of Cd^{2+} (10 μM) increase the observed non-uniformity of the first stimulated $[Ca^{2+}]_i$-transient. This concentration of Cd^{2+} is an order of magnitude below that required to block 50% of the sodium current and does not

inhibit the Na/Ca exchanger (Sheets and Hanck, 1992; Egan et al., 1989; Frame and Milanick, 1991). It has been suggested that calcium influx via the exchanger, stimulated by the sodium current and depolarization, may be capable of triggering calcium release (Leblanc and Hume, 1990; Levi et al., 1993). Thus in these conditions, we would have expected any possible contribution of the Na/Ca exchanger to E-C coupling to have been hardly affected. Because some regions of the cell failed to release calcium in response to depolarization in the presence of a low concentration of Cd^{2+}, we conclude that the Na/Ca exchanger does not appear to play a major role in triggering calcium release from the SR. Instead, our results are more simply explained by the SR release being triggered by L-type calcium channels and by Cd^{2+} simply reducing the probability of SR release channel opening at all points within the cell (rather than a reduction in the amplitude of SR release at all points within the cell).

Cd^{2+} is a fast open channel blocker (i.e., it reduces t_{open}), which leaves the single-channel conductance unaltered (Lansman et al., 1986), so that the observation that there is a reduction in the number of sites that release calcium in these conditions supports the idea that the stochastic gating of the L-type calcium channel is a major factor in determining the pattern of calcium release. Although direct evidence for non-uniformities in the trigger calcium influx was limited by the signal-to-noise ratio in our data, it is likely that non-uniformities in the timing of L-type calcium opening is an important factor in determining when calcium release by the SR occurs. These data also suggest that the open time of the DHPR is an important determinant of the probability of SR calcium release channel opening.

The relationship between the open time of the DHPR and the SR calcium release may not be linear, because the local calcium concentration will eventually reach some steady state with longer-lasting openings (i.e., the temporal relationship between local calcium influx and SR release should show saturation). Our results obtained with Cd^{2+} suggest that the open time of the DHPR is not so long that E-C coupling operates in a saturated condition. This arises from the observation that the probability of calcium release is reduced by reducing the mean open time of the DHPR (with Cd^{2+}). In addition, we expect the probability of release unit activation to decline at more positive potentials (for a given DHPR open time), because voltage also affects the flux through the DHPR. In connection with these points, Cannell et al. (1987) showed that SR calcium release appeared to be near maximal over a range of voltages where the calcium current could be increased by as much as 50%. In addition, it was shown that 30% of the maximal calcium current caused 83% of the maximum SR release at negative membrane potentials, whereas 60% was released at positive potentials (their Fig. 3).

More recently, Wier et al. (1994) have extended some of the results of Cannell et al. (1987) and have concluded that local non-uniformities in $[Ca^{2+}]_i$ may be the cause of the apparent variation in the ability of a given calcium current to cause calcium release from the SR (or variation in gain as defined by the flux ratio; see below). However, it should be noted that their conclusions are based on the interpretation of spatially averaged data obtained with a highly nonlinear calcium indicator (indo-1), which will cause errors in estimating $[Ca^{2+}]_i$ when spatial non-uniformities in $[Ca^{2+}]_i$ are present (Yue and Wier, 1985). Unfortunately, although we have demonstrated that non-uniformities in $[Ca^{2+}]_i$ are present during the rising phase of the $[Ca^{2+}]_i$ transient, we are unable to quantify the possible contamination of the data of Wier et al. (1994) by nonlinear indicator effects. Nevertheless, it is clear that caution should be applied to the interpretation of experiments that depend on measuring (with nonlinear indicators) $[Ca^{2+}]_i$ during the rising phase of the $[Ca^{2+}]_i$ transient, especially when the calcium current is reduced, as gross non-uniformities in $[Ca^{2+}]_i$ then occur.

Relationship between the increased calcium spark rate during E-C coupling and the trigger calcium influx

During E-C coupling, our data suggest that there is a large increase in the calcium spark rate to $\sim 144\ s^{-1}\ \mu m^{-1}$. Under resting conditions, the spontaneous calcium spark rate is about $1\ s^{-1}$ in a line-scan image encompassing 150 μm (data not shown; Cheng et al., 1993), which implies that the trigger calcium influx increased the spark rate by about 2.2×10^4. If the calcium spark rate is determined only by the local calcium concentration (as required by the CICR mechanism), this implies that this increase in rate should be proportional to the increment in local calcium raised to the power N, where N is the apparent number of calcium sites that regulate release channel opening. If the opening rate of the RyR is proportional to the square of the local calcium concentration ($N = 2$; see Györke and Fill, 1993, Fig. 2), then a 2.2×10^4 increase in calcium spark rate would require local calcium to increase by a factor of about 150. Thus if the resting calcium concentration is 100 nM, the local calcium concentration would have to increase to $\sim 15\ \mu M$ to explain the observed increase in calcium spark rate (note that a linear dependence of RyR opening rate on $[Ca^{2+}]_i$ is not compatible with these data). This predicted increase in local calcium concentration is considerably greater than the estimate of the increase in spatial averaged calcium (34 nM) observed in the presence of SR inhibitors.

The difference between these two figures can be explained by the calcium influx entering and being sensed in a "fuzzy space" (Niggli and Lederer, 1990a; Lederer et al., 1990) from which the calcium subsequently diffuses. Assuming that the calcium influx into the fuzzy space is the same as that which appears in the cytoplasm, these observations suggest that the fuzzy space (i.e., the volume in which the trigger calcium is sensed) must be <0.2% of the cytoplasmic volume (this is an upper-limit estimate, given that it ignores calcium uptake and the time course of calcium influx during the action potential). This is similar to an estimate of the volume of the "fuzzy space" (0.3%; Lederer et al., 1990) and, for comparison, is of the same order as that of the junctional SR (0.3% of cell

volume (Page et al., 1971)). Thus our data support the idea that the trigger calcium initially flows into a small fraction of the cell (or fuzzy space) where it is sensed by the CICR mechanism to cause release from the SR (see Niggli and Lederer, 1990a; Lederer et al., 1990; Leblanc and Hume, 1990; Sham et al., 1992). Thus the close apposition of the SR and t-tubular membranes ensures that when an L-type calcium channel opens the SR calcium release channels are exposed to a high calcium concentration to greatly increase their opening rate. Although once opened the SR release channel will activate its neighbors, the system does not exhibit uncontrolled regenerative behavior (i.e., the SR release channels do not remain permanently open) because the finite open time of the RyR ensures that the SR release channels will eventually close and allow diffusion of the activator calcium to reduce the local calcium concentration below a level needed to reactivate the SR release channel(s). This process has been termed "stochastic attrition" (Stern, 1992) and provides both high gain as well as stability in E-C coupling.

Calcium release during steady-state contractions

In rat heart muscle, steady-state contractions are smaller than rested-state contractions, a phenomenon that may be due to a reduction in the calcium content of the SR (see Bers (1991) for review). In principle, the decreased amplitude of the $[Ca^{2+}]_i$ transient and contraction strength could arise from two mechanisms: first, a reduction in the number of SR release channels that open with each depolarization; and second, a reduced calcium flux from each open channel as a result of the decrease in SR lumenal calcium concentration. Considering the first possibility, there are several lines of evidence (albeit indirect) that support such a mechanism. 1) In vesicles, the calcium release rate-constant depends on the occupation of calsequestrin by calcium (Ikemoto et al., 1989). 2) Bilayer experiments suggest that the p_o of the SR Ca-release channel is increased by lumenal Ca^{2+} (Thedford et al., 1994; Tripathy and Meissner, 1994). 3) Ryanodine alters the transition between low- and high-affinity states of an intralumenal calcium-binding protein that may be calsequestrin (Gilchrist et al., 1992). 4) Calsequestrin removal abolishes calcium transients inside the SR lumen as well as calcium release (Ikemoto et al., 1989, 1991). These lines of evidence suggest that the lumenal calcium and the calcium occupancy of calsequestrin (and hence its conformation) plays some role in the regulation of the ryanodine receptor. Thus the depletion of calcium from calsequestrin during the negative staircase could reduce the probability of the release channel opening, but our data do not show an increase in the non-uniformity of $[Ca^{2+}]_i$ in these conditions. However, it is not possible to exclude such a mechanism at the present time, given that the calcium current increases during the staircase from rest (Hryshko and Bers, 1991), which might offset a possible decrease in open probability. It is also possible that regulation of the SR release channel by the calcium level in the SR lumen is only apparent when the SR calcium content is quite different from that occurring in these experiments.

Nevertheless, our data show that the level of free calcium in the SR lumen must be lower during repetitive stimuli (given that the flux was reduced while the number of release sites was approximately the same). This observation raises the possibility that the free calcium level in the SR lumen becomes significantly reduced during a normal $[Ca^{2+}]_i$ transient. In support of this possibility, it has been suggested that the maximum calcium content of the SR is comparable to the amount of calcium required for a normal contraction (Jorgensen et al., 1988; Varro et al., 1993; Bassani et al., 1993).

Calcium fluxes and coupling between the DHPR and RyR

As pointed out earlier, the total flux from the SR is ~40 times that of the calcium current and other membrane fluxes. The flux (J) through an identified channel population is proportional to $p_o \cdot i \cdot n$ (where n is the number of channels and i the single-channel current). Thus the flux ratio over the entire calcium transient would be:

$$\frac{\overline{J_R}}{\overline{J_D}} = \frac{\overline{p_{o(R)}} \cdot i_R \cdot n_R}{\overline{p_{o(D)}} \cdot i_D \cdot n_D} \tag{8}$$

(R referring to RyR and D to DHPR). Given $n_R/n_D = 7$ (Bers and Stiffel, 1993) and $i_R/i_D = 7$ ($i_R = 2.2$ pA (Rousseau and Meissner, 1989); $i_D = 0.31$ pA (Rose et al., 1992)), we can estimate that $p_{o(R)}/p_{o(D)} = 0.8$, so that the average open probability of the RyR during the entire calcium transient would be comparable to that of the DHPR. However, this does not imply that the gain of E-C coupling is low, because the stochastic gating of the calcium channels involved in E-C coupling is inadequately described by their p_o. In connection with this point, we note that because the time course of calcium spark activation closely matches the latency to first opening probability density function of L-type calcium channels (see above), it is likely that 1) the time course of E-C coupling is determined by the time course of L-type calcium channel gating, and 2) the probability of release unit activation by an L-type calcium channel opening is very high under normal physiological conditions. Such close coupling between the functional calcium release unit and the L-type calcium channel will be helped by the clustering of RyRs into functional units. For example, if the functional unit contains four RyRs (as suggested above) then the probability of unit activation will be up to four times greater than the probability of a single RyR opening (depending on p_{open} of the RyR). It is intriguing to note that this clustering of RyRs into functional units will tend to oppose any possible decrease in p_{open} of the individual RyRs from reducing the probability of SR calcium release unit activation.

At a simplistic level, the ratio of fluxes (40) could also be described as the gain of E-C coupling, but given that the transfer function between input and output is not continuous, caution must be applied to any interpretation of such a

measure. To clarify the latter point, consider that the sarcolemmal calcium channels open before the SR release channels so that the ratio of single-channel fluxes is initially 0. Later, the sarcolemmal calcium channels close while the SR channels are open, so that the ratio of single-channel fluxes is infinite. Thus the gain of E-C coupling at the level of the elementary local events goes from 0 to infinity during the contraction and between contractions, when both channels are closed, and the ratio of fluxes is indeterminate. Such behavior is inconsistent with continuous (analog gain) models of E-C coupling, so that it will be necessary to consider stochastic behavior in future models of E-C coupling to adequately describe behavior at sarcomeric and subsarcomeric levels.

The problem of defining a single figure of merit for the strength of E-C coupling has been appreciated in other studies of E-C coupling where it was noted that the gain of E-C coupling appeared to be variable depending on the voltage protocol that was used to elicit calcium release from the SR (Cannell et al., 1987b; Niggli and Lederer, 1990; Wier et al., 1994). Indeed, this problem led Cannell et al. (1987b) to suggest that E-C coupling may be mediated by a process that requires calcium influx but that might be modulated by voltage. A direct role of voltage was ruled out by experiments using caged calcium (Niggli and Lederer, 1990b), but it is clear that voltage can affect E-C coupling by modulating both the single-channel flux and mean open time of the sarcolemmal calcium channel. With these two variables being independent and both having nonlinear effects on SR release channel activation, the apparently variable gain of E-C coupling (in the flux-ratio sense) can be explained on the basis of local stochastic behavior described here.

Supported by grants from the National Institutes of Health (HL36974, HL26975), DRIF awards from the University of Maryland at Baltimore, and support from the Medical Biotechnology Center and the British Heart Foundation.

REFERENCES

Allen, D. G., D. A. Eisner, and C. H. Orchard. 1984. Factors influencing free intracellular calcium concentration in quiescent ferret ventricular muscle. *J. Physiol.* 350:615–630.

Barcenas-Ruiz, L., and W. G. Wier. 1987. Voltage dependence of intracellular Ca^{2+} transients in guinea pig vetricular myocytes. *Circ. Res.* 61:148–154.

Bassani, J. W. M., R. A. Bassani, and D. M. Bers. 1993. Twitch-dependent SR Ca accumulation and release in rabbit ventricular myocytes. *Am. J. Physiol. Cell Physiol.* 265:C533–C540.

Berlin, J. R., M. B. Cannell, and W. J. Lederer. 1989. I_{Ti} in single rat cardiac ventricular cells: relationship to fluctuations in intracellular calcium. *Circ. Res.* 65:115–126.

Beukelmann, D. J., and W. G. Wier. 1988. Mechanism of calcium release from sarcoplasmic reticulum of guinea-pig cardiac cells. *J. Physiol.* 405: 233–255.

Bers, D. M. 1991. Excitation-contraction coupling and cardiac contractile force. Kluwer Academic Publishers, The Netherlands.

Bers D. M., J. H. Bridge, and K. W. Spitzer. 1989. Intracellular Ca^{2+} transients during rapid cooling contractures in guinea-pig ventricular myocytes. *J. Physiol.* 417:537–553.

Bers, D. M., and Stiffel, V. M. 1993. Ratio of ryanodine to dihydropyridine receptors in cardiac and skeletal muscle. *Am. J. Physiol.* 264: C1587–1593.

Blanchard, E. M., G. L. Smith, D. G. Allen, and N. R. Alpert. 1990. The effects of 2,3-butanedione monoxime in initial heart, tension and aequorin light output of ferret papillary muscles. *Pfluegers Arch.* 416:219–221.

Bouchard, R. A., and D. Bose. 1992. Contribution of sarcolemmal sodium-calcium exchange and intracellular calcium release to force development in isolated canine ventricular muscle. *J. Gen. Physiol.* 99:931–960.

Bouchard, R. A., and D. Bose. 1989. Analysis of the interval-force relationship in rat and canine ventricular myocardium. *Am. J. Physiol.* 257: H2036–H2047.

Callewaert, G. 1992. Excitation-contraction coupling in mammalian heart cells. *Cardiovasc. Res.* 26:923–932.

Callewaert, G., L. Cleeman, and M. Morad. 1988. Epinephrine enhances Ca^{2+} current-regulated Ca^{2+} release and Ca^{2+} uptake in rat ventricular myocytes. *Proc. Natl. Acad. Sci. USA.* 85:2009–2013.

Cannell, M. B. 1991. Contribution of sodium-calcium exchange to calcium regulation in cardiac muscle. *Ann. N. Y. Acad. Sci.* 639:428–443.

Cannell, M. B., and D. G. Allen. 1984. A model of calcium movements during activation in the sarcomere of frog skeletal muscle. *Biophys. J.* 45:913–925.

Cannell, M. B., J. R. Berlin, and W. J. Lederer. 1987a. Intracellular calcium in cardiac myocytes: calcium transients measured using fluorescence imaging. *In* Cell Calcium and Control of Membrane Transport. L. J. Mandel and D. C. Eaton, editors. Rockefeller University Press, New York. 201–214.

Cannell, M. B., J. R. Berlin, and W. J. Lederer. 1987b. Effect of membrane potential changes on the calcium transient in single rat cardiac muscle cells. *Science.* 238:1419–1423.

Cheng, H., W. J. Lederer, and M. B. Cannell. 1993. Calcium sparks: elementary events underlying excitation-contraction coupling in hear muscle. *Science.* 262:740–744.

Cleeman, L., and M. Morad. 1991. Role of Ca^{2+} channel in cardiac excitation-contraction coupling in the rat: evidence from Ca^{2+} transients and contraction. *J. Physiol.* 432:283–312.

duBell, W. H., and S. R. Houser. 1989. Voltage and beat dependence of Ca^{2+} transient in feline ventricular myocytes. *Am. J. Physiol.* 257:H746–759.

Egan, T. M., D. Noble, S. J. Noble, T. Powell, A. J. Spindler, and V. W. Twist. 1989. Sodium-calcium exchange during the action potential in guinea-pig ventricular cells. *J. Physiol.* 411:639–661.

Fabiato, A. 1985a. Simulated calcium current can both cause calcium loading in and trigger the calcium release from the sarcoplasmic reticulum of a skinned cardiac cell. *J. Gen. Physiol.* 85:291–320.

Fabiato, A. 1985b. Time and calcium dependence of activation and inactivation of calcium-induced calcium release of calcium from the sarcoplasmic reticulum of a skinned cardiac Purkinje cell. *J. Gen. Physiol.* 85:247–290.

Frame, M. D. S., and M. S. Milanick. 1991. Mn and Cd transport by the Na-Ca exchanger of ferret red blood cells. *Am. J. Physiol.* 261: C467-C475.

Gilchrist, J. S., A. N. Belcastro, and S. Katz. 1992. Intraluminal Ca^{2+} dependence of Ca^{2+} and ryanodine-mediated regulation of skeletal muscle sarcoplasmic reticulum Ca^{2+} release. *J. Biol. Chem.* 267:20850–20856.

Grynkiewicz, G., M. Poenie, and R. Y. Tsien. 1985. A new generation of Ca^{2+} indicators with greatly improved fluorescence properties. *J. Biol. Chem.* 260:3440–3450.

Gwamathey, J. K., R. J. Hajjar, and R. J. Solaro. 1991. Contractile deactivation an uncoupling of crossbridges. Effect of 2,3-butanedione monoxime on mammalian myocardium. *Circ. Res.* 69:1280–1292.

Györke, S., and M. Fill. 1993. Ryanodine receptor adaptation: control mechanism of Ca^{2+}-induced Ca^{2+} release in heart. *Science.* 260:807–809.

Györke, S., C. Dettbarn, and P. Palade. 1993. Potentiation of sarcoplasmic reticulum Ca^{2+} release by 2,3-butanedione monoxime in crustacean muscle. *Pfluegers Arch.* 424:39–44.

Hryshko, L. V., and D. M. Bers. Ca current facilitation during postrest recovery depends on Ca entry. *Am. J. Physiol.* 259:H951-H961.

Ikemoto, N., M. Ronjat, L. G. Measzaros, and M. Koshita. 1989. Postulated role of calsequestrin in the regulation of calcium release from the sarcoplasmic reticulum. *Biochemistry.* 28:6764–6771.

Ikemoto, N., B. Antoniu, J. J. Kang, L. G. Mesazoros, and M. Ronjat. 1991. Intravesicular calcium transient during calcium release from sarcoplasmic reticulum. *Biochemistry.* 30:5230–5237.

Jorgensen, A. O., A. C.-Y. Shen, and K. P. Campbell. 1985. Ultrastructural localization of casequestrin in adult rat atrial and ventricular muscle cells. *J. Cell. Biol.* 101:257–268.

Jorgensen, A. O., R. Broderick, A. P. Somlyo, and A. V. Somlyo. 1988. Two structurally distinct calcium storage sites in rat cardiac sarcoplasmic reticulum: an electron microprobe study. *Circ. Res.* 63: 1060–1069.

Jorgensen, A. O., A. C. Shen, W. Arnold, P. S. McPherson, and K. P. Campbell. 1993. The Ca^{2+}-release channel/ryanodine receptor is localized in junctional and corbular sarcoplasmic reticulum in cardiac muscle. *J. Cell Biol.* 120:969–80

Kirby, M. S., Y. Sagara, S. Gaa, G. Inesi, W. J. Lederer, and T. B. Rogers. 1992. Thapsigargin inhibits contraction and Ca^{2+} transient in cardiac cells by specific inhibition of the sarcoplasmic reticulum Ca^{2+} pump. *J. Biol. Chem.* 267:12545–12551.

Lansman, J. B., P. Hess, and R. W. Tsien. 1986. Blockade of current through single calcium channels by Cd^{2+}, Mg^{2+}, and Ca^{2+}. *J. Gen. Physiol.* 88: 321–347.

Leblanc, N., and J. R. Hume. 1990. Sodium current-induced release of calcium from cardiac sarcoplasmic reticulum. *Science.* 248:372–376.

Lederer, W. J., E. Niggli, and R. W. Hadley. 1990. Sodium-calcium exchange in excitable cells: fuzzy space. *Science.* 248:283.

Levi, A. J., P. Brooksby, and J. C. Hancox. 1993. A role for depolarization induced calcium entry on the Na-Ca exchange in triggering intracellular calcium release and contraction in rat ventricular myocytes. *Cardiovasc. Res.* 27:1677–1690.

Lew, W. Y., L. V. Hryshko, and D. M. Bers. 1991. Dihydropyridine receptors are primarily functional L-type calcium channels in rabbit ventricular myocytes. *Circ. Res.* 69:1139–1145.

Li, T., N. Sperelakis, R. E. Teneick, and J. Solaro. 1985. Effects of diacetyl monoxime on cardiac excitation-contraction coupling. *J. Pharmacol. Exp. Ther.* 232:688–695.

Melzer, W., E. Rios, and M. F. Schneider. 1987. A general procedure for determining the rate of release from the sarcoplasmic reticulum in skeletal muscle fibers. *Biophys. J.* 51:849–863.

McGuigan, J. A. S., and J. A. Blatter. 1987. Sodium/calcium exchange in ventricular muscle. *Experimentia.* 43:1140–1145.

McPherson, P. S., and K. P. Campbell. 1993. The ryanodine receptor/Ca^{2+} release channel. *J. Biol. Chem.* 268:13765–13768.

Minta, A., J. P. Kao, and R. Y. Tsien. 1989. Fluorescent indicators for cytosolic calcium based on rhodamine and fluorescence chromophores. *J. Biol. Chem* 264:8171–8178.

Mitra, R., and M. Morad. 1985. A uniform enzymic method for dissociation of myocytes from hearts and stomachs of vertebrates. *Am. J. Physiol.* 246:H1056-H1060.

Niggli, E., and W. J. Lederer. 1990a. Voltage-independent calcium release in heart muscle. *Science.* 250:565–568.

Niggli, E., and W. J. Lederer. 1990b. Real-time confocal microscopy and calcium measurements in heart muscle cells: towards the development of a fluorescence microscope with high temporal and spatial resolution. *Cell Calcium.* 11:121–130.

O'Niell, S. C., J. G. Mill, and D. A. Eisner. 1990. Local activation of contraction in isolated rat ventricular myocytes. *Am. J. Physiol.* 258: C1165–1168.

Page, E., L. P. McCallister, and B. Power. 1971. Stereological measurements of cardiac ultrastructures implicated in excitation-contraction coupling. *Proc. Natl. Acad. Sci. USA.* 68:1465–1466.

Rousseau, E., and G. Meissner. 1989. Single cardiac sarcoplasmic reticulum Ca^{2+}-release channel: activation by caffeine. *Am. J. Physiol.* 256:H328-H333.

Rose, W. C., C. W. Balke, W. G. Wier, and E. Marban. 1992. Macroscopic and unitary properties of physiological ion flux through L-type Ca^{2+} channels in guinea-pig heart cells. *J. Physiol.* 456:267–284.

Sham, J. S. K., L. Cleeman, and M. Morad. 1992. Gating of the cardiac Ca^{2+} release channel: the role of Na^+ current and Na^+-Ca^{2+} exchange. *Science.* 255:850–853.

Sheets, M. F., and D. A. Hanck. 1992. Mechanisms of extracellular divalent and trivalent cation block of the sodium current in canine cardiac Purkinje cells. *J. Physiol.* 454:299–320.

Sipido, K. R., and W. G. Wier. 1991. Flux of Ca^{2+} across the sarcoplasmic reticulum of guinea-pig cardiac cells during excitation contraction coupling. *J. Physiol.* 435:605–630.

Steele, D. S., and G. L. Smith. 1993. Effects of 2,3-butanedione monoxime on sarcoplasmic reticulum of saponin-treated rat cardiac muscle. *Am. J. Physiol.* 265:H1493-H1500.

Stern, M. D. 1992. Theory of excitation-contraction coupling in cardiac muscle. *Biophys. J.* 63:497–517.

Stewart, J. M., and E. Page. 1978. Improved stereological techniques for studying myocardial cell growth: application to external sarcolemma, T system, and intercalated disks of rabbit and rat hearts. *J. Ultrastruct. Res.* 65:119–134.

Takamatsu, T., and W. G. Wier. 1990a. Calcium waves in mammalian heart: quantification of origin, magnitude, waveform and velocity. *FASEB J.* 4:1519–1525.

Takamatsu, T., and W. G. Wier. 1990b. High temporal resolution video imaging of intracellular calcium. *Cell Calcium.* 11:111–120.

Thedford, S. E., W. J. Lederer, and H. H. Valdivia. 1994. Activation of sarcoplasmic reticulum calcium release channels by intraluminal Ca^{++}. *Biophys. J.* 66:A20.

Trafford, A. W., S. C. O'Niell, and D. A. Eisner. 1993. Factors affecting the propagation of locally activated systolic Ca transients in rat ventricular myocytes. *Pfluegers Arch.* 425:181–183.

Tripathy, A., and Meissner, G. 1994. Effect of SR lumenal Ca^{++} on the open probability of the skeletal muscle ryanodine receptor/Ca^{++} release channel. *Biophys. J.* 66:A416.

Varro, A., N. Negretti, S. B. Hester, and D. A. Eisner. 1993. An estimate of the calcium content of the sarcoplasmic reticulum in rat ventricular myocytes. *Pfluegers Arch.* 423:158–160.

Wier, W. G. 1990. Cytoplasmic calcium in the mammalian ventricle: dynamic control by cellular processes. *Annu. Rev. Physiol.* 52:467–485.

Wier, W. G., M. B. Cannell, J. R. Berlin, E. Marban, and W. J. Lederer. 1987. Cellular and subcellular heterogeneity of $[Ca^{2+}]_i$ in single heart cells revealed by fura-2. *Science.* 235:325–328.

Wier, W. G., T. M. Egan, J. R. Lopez-Lopez, and C. W. Balke. 1994. Local control of excitation-contraction coupling in rat heart cells. *J. Physiol.* 474:463–471.

Wier, W. G., and D. T. Yue. 1986. Intracellular calcium transients underlying the short-term force-interval relationship in ferret ventricular myocardium. *J. Physiol.* 376:507–530.

Wilbo, M., and T. Godfraind. 1991. Stoichiometric ratio of calcium entry to calcium release channels in rat ventricle in relation to the mechanism of sarcoplasmic reticulum calcium release in cardiac tissue. *Pfluegers Arch.* 419:R13.

Yue, D. T., and W. G. Wier. 1985. Estimation of intracellular calcium by non-linear indicators. *Biophys. J.* 48:533–537.